Al-Sibd Center for Research and Scholarly Publishing
Journal of Energy Sustainability and Economics (JESE)
Journal Homepage : https://jese.srp-center.iq/

New Approach For The Performance of Reservoirs Depleted by Long Horizontal Wellbores With Closed Sections

Ahmed M. Aljarah

University of Kerbala, Iraq

Corresponding Author : Ahmed.musa@buog.edu.iq

Keywords:

Horizontal Wells; Reservoirs Performance; Reservoirs modeling ;pressure behavior; flow regimes;

Abstract

This paper introduces a new approach for reservoir performance where long horizontal wellbores are extended in the porous media with the existence of closed sections. It focuses on the impact of these sections on the pressure behavior, flow regimes, and productivity index considering different characteristics for the closed sections in terms of the length and petrophysical properties. New analytical solutions for the flow equations are presented wherein three porous media are considered in the rectangular closed reservoirs of different configurations. The methodology used in this approach includes different tasks. The first is developing analytical models for the pressure drop caused by the production at a constant sandface flow rate from a horizontal wellbore where a part of it is closed. These models are developed based on the fact that the porous media with the existence of the closed sections in the horizontal wellbores consists of three regions. The first represents the porous media in the vicinity of the open section of the wellbore and extends to a distance equal to half the formation thickness while the second is the porous media of the open section that extends beyond the first region and reaches the reservoir boundary. The third region represents the porous media of the closed sections that extend from the wellbore to the reservoir boundary. In the second task, the proposed models are solved for different reservoir configurations, wellbore lengths, and closed and open section characteristics. The impact of closed sections on transient and stabilized pseudo-steady state productivity indices are demonstrated in third tacks while the analytical models of the observed flow regimes in the porous media are presented in the fourth task with a major focus given to those impacted by the closed sections. The results of the developed models are verified by the comparison with the results obtained from the available well-known models in the literature. The outcomes of this study can be summarized in the following points: 1) The pressure behavior, flow regimes, and productivity index are significantly influenced by the existence of closed sections. This influence is significant during early production time, but it decreases during intermediate production, however, it is not seen at late production time. 2) The impact of closed sections becomes more severe when the petrophysical properties of the closed sections are greatly different from those of open sections. 3) The pressure behavior of early production time is not affected by the petrophysical properties of the closed section porous media while pseudo-steady state flow is significantly impacted by these properties. 4) The pressure and pressure derivative behaviors of long horizontal wellbores with long closed sections are similar to those developed in reservoirs depleted by hydraulic

fractures. 5) Reaching pseudo-steady state flow may need a longer time when there is a great difference in the petrophysical properties between closed and open sections, however, the length of the closed sections may not have such impact. Two novel points are reached in this study. The first is developing new analytical models for the pressure behavior of reservoirs depleted by horizontal wellbores with closed sections. The second is observing a new bi-linear flow regime instead of linear flow regime. This flow regime represents simultaneous linear flow from the closed section porous media to the open section and from the open section to the porous media in the vicinity of the open section of the wellbore. New analytical models for the pressure and pressure derivative of this flow regime is introduced in this study.

Introduction

Horizontal wells have been a successful application for developing oil and gas fields in the last decades due to their capabilities to enhance significantly reservoir performance and increase drastically the production capacity. Extending to a large areal extent of hydrocarbon accumulations that would increase the cross-section area of flow from the porous media to the wellbores as well as the beneficial usage of the vertical permeability are the two main objectives of this application. Extra benefits of the horizontal wells are represented by the less turbulent conditions in the vicinity of the wellbore as the convergence of the flow streamlines is not severe, the reasonable control of water and gas coning, and the possibility to intersect more naturally induced fractures that would increase well's deliverability.

The completion system of a horizontal well is of great importance due to its impact on the deliverability either in the early or late production time. Accordingly, the selection of the completion type is a crucial decision not only in terms of the expected production capacity but also for the well integrity and stability. The competence of the formations and the borehole collapse because of the shear failure that is often very severe in horizontal wells as well as the sand production from unconsolidated layers are considered carefully when it comes to choosing the completion type. It is very well documented that the horizontal wells are completed by one of four types: open hole, slotted liner, casing packers, and cemented casing. Economically, the open hole completion is a good candidate for the consolidated formations, however, it does not give the operators the opportunities to perform diagnostics or remedial works when they are needed (Rentano and Muhammed 1999). The other three types of completion can be utilized when the open hole completion does not fulfill the required functions. Slotted linear or perforated linear may not provide different flexibility, production control, and stimulation plans than the open hole completion (Seale et al. 2007). The external casing packers and the cemented casing are more flexible for the production and fluid placement during stimulation. Both completion techniques may have sections from the horizontal wellbores that are not open to flow.

In this study, a deep focus is given to these two techniques wherein the impacts of the closed sections of the horizontal wellbores on the pressure behavior, flow regimes, and productivity index are profoundly investigated. The closed sections might be implemented either by utilizing zonal isolations where the horizontal wellbores are segmented by external casing packers and blank liners that could be interspersed along the slotted or perforated liners. Cased and cemented holes are selectively perforated also for different reasons such as reducing the cost, delaying premature water/gas breakthrough, preventing wellbore collapse in the unstable sections of the formations, and producing multiple zones with high productivity contrast (Yildiz 2004, Yildiz 2006). There are several field applications for selectively perforated horizontal wells. Horn et al. 1998 stated that multizone completion was used for dual-lateral horizontal wells drilled in the Bongkot field in Thailand. This technique helped reducing gas and water production and increasing oil recovery by shutting the sections where gas and water were produced. In the same year, multiple acid fracturing stimulation has been used by one of the operators of Joanne filed in the North Sea where 10 different zones were stimulated in a single trip with no intervention (Thomson and Nazroo 1998).

The partially completed or selectively perforated horizontal wellbores were experienced in the Oseberg field located in the Norwegian sector of the North Sea (Sognesand et al. 1994). The wells were completed using cemented liners where the inflow profile is controlled by the selective perforations. They were evaluated after four years of production and it has been found that the selective perforation technique has increased the production flexibility and improved zonal drainage (Sognesand 1996). The horizontal wells drilled in Statfjord field in the North Sea located on the Norwegian/UK borders were completed using cemented liners. These wells penetrate several zones that have to be produced selectively (Kostøl 1995). While the horizontal wells of Elk Hills in California, USA were completed using cemented external casing packers, cemented casing, and external casing packers. These completion techniques have been designed to successfully isolate the sand production intervals (Gangle et al. 1995).

The other field applications for partially completed and selectively perforated horizontal wells are those used in horizontal wells extended western area of the Prudhoe Bay, the largest Alaskan oil field to prevent gas production (Pucknell and Broman 1994). While Alpha and Bravo platforms have been used to deplete Beryl Field in the North Sea using multilateral horizontal wellbores where the completion system is designed to access the production from the original mother bore (Sadek et al. 1998). The sand production risk from the Varg Field located in the central part of the North Sea was minimized by adopting a perforation strategy wherein the direction of the perforations prevents sand production (Eriksen et al. 2001; Tronvoll et al. 2004). Hillestad et al. 2004 confirmed that the oriented perforation system used in the North Sea is important when the integrity of the formation is questionable and to sustain the production without sand production problems. The long horizontal wells used in Al Shaheen Field located on the central axis of the Qatar Arch have been segmented so that each segment can be controlled individually and to manage the offtake and injection along these wells (Abbasy et al. 2010).

The abovementioned literature review gives several examples where the completion systems of the horizontal wells may have open and closed sections. However, the objective of this paper is to study the impact of the closed sections on the pressure behavior and flow regimes of horizontal wellbores. Unfortunately, there are not many presented or published research papers that have been focused on this topic. Goode and Wilkinson 1991 probably the first who introduced a study for the impact of closed sections in the horizontal wells on the performance of rectangular bounded reservoirs. They have concluded that the wellbore length can be reduced without substantial change in the productivity index, and the uniformly distributed open sections along the wellbore could give better inflow performance. Later, Frick et al. 1995 published an article that targeted the well test analysis of a horizontal well with isolated segments. The main focus in this paper is given to the impact of the isolated segments on the skin factor and the impact of the effective wellbore length (open sections) on the pressure behavior and flow regimes. Four flow regimes have been observed in this study, early radial, linear, pseudo-radial, and pseudo-steady state flow regimes. A study for the transient pressure behavior of perforated slanted and horizontal wells was presented by Ozkan and Yildiz 1999 at which an intermediate radial flow regime is observed. This flow regime, according to the authors, is developed only for slanted wells and represents the flow radially in the vertical plan normal to the horizontal well and akin to the early radial flow regime of open hole horizontal wellbores.

The inflow performance relationships (IPR) of a horizontal well that was completed with randomly distributed perforation along the wellbore was presented by Yildiz 2004. The effects of the formation damage, crushing around perforation tunnels, shot phasing and density, perforation characteristics on the IPR were investigated by the author. Two years later, the productivity of selectively perforated horizontal wells was studied by Yildiz 2006. The author confirmed that the ratio of the total perforated length to the drilled length of the wellbore is the most dominant parameter controlling the long-term performance. The impact of the number and length of the zonal isolations on the pressure behavior and flow regimes of a horizontal well acting in a closed rectangular reservoir was demonstrated by Al-Rbeawi and Tiab 2012. They have reached a conclusion that two radial flow regimes could be observed at early production time. The first is the radial flow in the vertical plan toward each open section and the second is the radial flow in the horizontal plan toward each open section when the closed sections are larger than the open sections.

In the abovementioned literature review for the impact of the completion system on the reservoir performance, the reservoirs have been considered consisting of a single drainage area where the reservoir fluids flow toward the open sections of the horizontal wellbores. In the current study, the reservoirs consist of three drainage areas. The first is the porous medium close to the wellbore where the radial flow in the vertical plan is the dominant flow regime. The second is the porous medium that extends beyond the first drainage area to the reservoir boundary. The flow in this part is linear in the normal direction to the horizontal wellbore. While the third is the porous media that extends from the closed sections to the reservoir boundary. The flow in this part is linear in the normal direction to the second drainage area and parallel to the wellbore. For each drainage area, the flow equations have been solved using different boundary conditions and an analytical model for the pressure drop inside the horizontal wellbores has been developed. Different reservoir configurations, wellbore length, open and closed section lengths, and petrophysical properties of open and closed sections have been considered in this study.

Mathematical modeling

Let us consider a horizontal well as shown in Fig. (1). The well length and wellbore radius are ($2L_W$) and (r_w). It extends in a closed rectangular reservoir. The two reservoir boundaries are (x_e), and (y_e) and the formation thickness is (h). The wellbore is completed such that two sections located at the right and left side of the wellbore are left closed and a single open section is used between the two closed sections. The length of each closed section is (L_C), and the length of the open section is ($2L_O$).

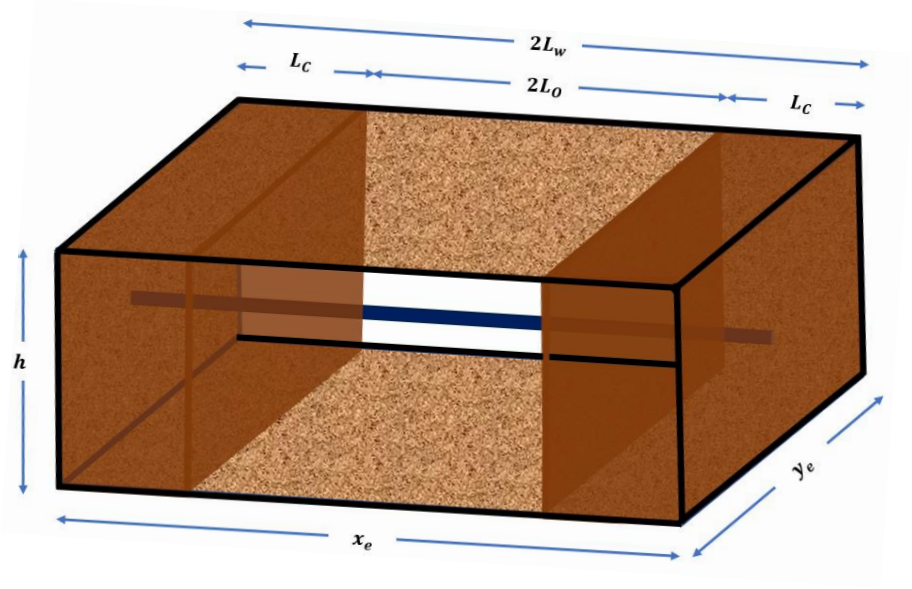

Figure 1: Horizontal well in a closed rectangular reservoir with closed sections.

The porous media of the reservoir, shown in Fig. (1), consists of three zones. The first is the porous media in the vicinity of the open section of the wellbore. This zone extends from the wellbore to a distance equal to $(h/2)$ in the direction of (y_e). The second zone is the porous media beyond the first zone and reaches the reservoir boundary (y_e). The third zone is the porous media in the vicinity of the closed sections and extends to the reservoir boundary (y_e). To solve the flow equations and develop an analytical model for the pressure drop inside the wellbore, the flow regimes that are expected to be observed in these three zones will be considered. For this purpose, the following assumptions have been considered:

1- The flow is a single-phase oil or gas.

2- The pressure drop caused by fluid flow inside the wellbore is not considered.

3- The wellbore extends symmetrically and horizontally in the horizontal plan from the midpoint in the vertical direction.

4- Constant flow rate.

5- The left and right-side closed sections are equal in length.

6- The formation is isotropic i.e. the permeability in the vertical and horizontal direction is the same and it has Uniform thickness.

The following are the main dimensionless parameters used in the study:

$$P_D = \frac{2\pi k_o h \Delta P}{q\mu B_o} \text{ for oil reservoirs} \quad (1)$$

$$t_D = \frac{k_o t}{(\emptyset \mu c_t)_o L_o^2} \quad (2)$$

$$x_D = \frac{x}{L_o} \quad (3)$$

$$x_{eD} = \frac{x_e}{L_w} \quad (4)$$

$$y_D = \frac{y}{L_w} \quad (5)$$

$$y_{eD} = \frac{y_e}{L_w} \quad (6)$$

$$L_D = \frac{L_w}{h} \quad (7)$$

$$L_{Do} = \frac{L_o}{h} \quad (8)$$

$$L_{Dc} = \frac{L_c}{h} \quad (9)$$

$$h_D = \frac{h}{L_w} \quad (10)$$

$$r_{wD} = \frac{r_w}{L_w} \quad (11)$$

All dimensionless parameters used in the manuscript is given in Appendix-A.

Third zone (closed sections)

This zone is determined by the porous media in the closed sections between the wellbore and the reservoir boundary (y_{eD}), and ($x_D = 1.0$) and (x_{eD}). The petrophysical properties in these sections are assumed different than the properties of the open section. Therefore;

$$\eta_D = \frac{\eta_c}{\eta_o} = \frac{k_c/(\emptyset\mu c_t)_c}{k_o/(\emptyset\mu c_t)_o} \quad (12)$$

The subscripts (o, c) mean open and closed sections respectively. The expected flow regime in the closed sections is a linear flow towards the second zone as it is shown in Fig. (2). The reservoir fluids flow parallel to the wellbore. The flow equation in the closed sections using Laplace domain, in dimensionless parameters is given by:

$$\frac{\partial^2 \bar{P}_{Dc}}{\partial x_D^2} - \frac{s}{\eta_D}\bar{P}_{Dc} = 0.0 \quad (13)$$

The two boundary conditions for this zone are:

$$\left.\frac{\partial \bar{P}_{Dc}}{\partial x_D}\right|_{x_D = x_{eD}} = 0.0 \quad (14)$$

$$\bar{P}_{Dc}|_{x_D=1.0} = \bar{P}_{Do}|_{x_D=1.0} \quad (15)$$

Eq. (13) can be solved using the two boundary conditions given by Eqs. (14), and (15).

$$\bar{P}_{Dc} = \bar{P}_{Do}|_{x_D=1.0} \frac{cosh[\sqrt{s/\eta_d}(x_{eD} - x_D)]}{cosh[\sqrt{s/\eta_d}(x_{eD} - 1.0)]} \quad (16)$$

where (P_{Dc}), and (P_{Do}) are the pressure in the closed (third zone) and open (second zone) sections respectively.

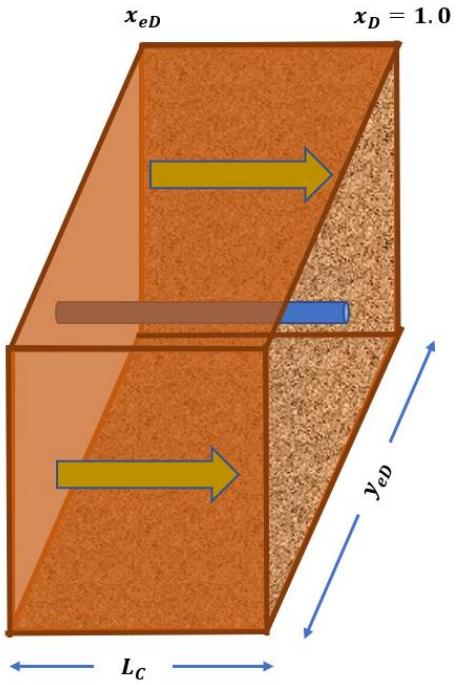

Figure 2 Third zone (closed section).

Second zone (open sections close to reservoir boundary)

The porous media in the second zone is determined by the space between reservoir boundary (y_{eD}) and a point located at a distance ($h_D/2$) from the wellbore as shown in Fig. (3). Reservoir fluids in this zone linearly flow towards the first zone (the vicinity of the open section of the wellbore). This zone receives reservoir fluids that come from the third zone. The flow equation in the second zone is given by:

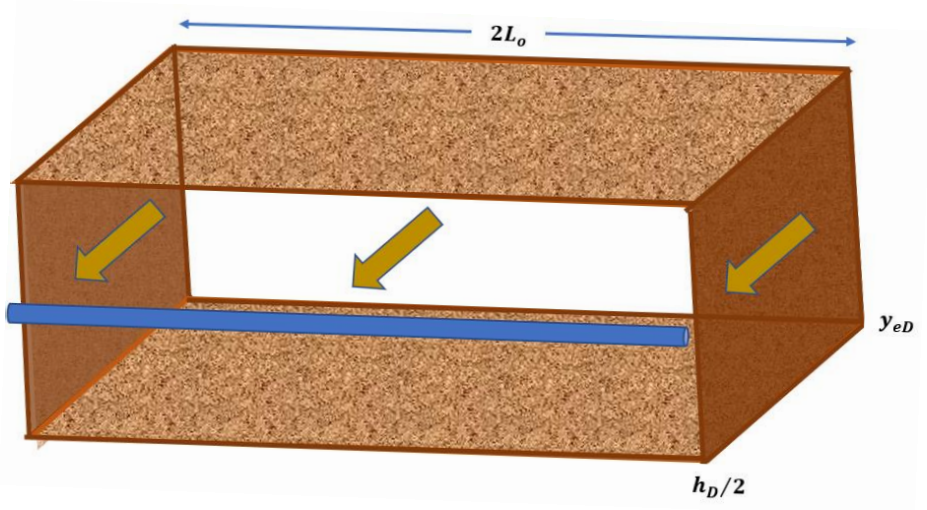

Figure 3 Second zone (porous media close to reservoir boundary).

$$\frac{\partial^2 \bar{P}_{Do}}{\partial y_D^2} + \frac{1}{y_{eD}\,\mathrm{M}_D}\frac{\partial \bar{P}_{Dc}}{\partial x_D}\Big|_{x_D=1.0} - s\bar{P}_{Do} = 0.0 \quad (17)$$

where:

$$\mathrm{M}_D = \frac{k_o}{k_c(y_{eD}-h_D/2)} \quad (18)$$

The two boundary conditions of the second zone are:

$$\frac{\partial \bar{P}_{Do}}{\partial y_D}\Big|_{y_D=y_{eD}} = 0.0 \quad (19)$$

$$\bar{P}_{Do}|_{y_D=h_D/2} = \bar{P}_{Dr}|_{y_D=h_D/2} \quad (20)$$

Using these to boundary conditions, Eq. (17) can be solved to:

$$\bar{P}_{Do} = \bar{P}_{Dr}|_{y_D=h_D/2}\frac{cosh[\sqrt{\delta}(y_{eD}-y_D)]}{cosh[\sqrt{\delta}(y_{eD}-h_D/2)]} \quad (21)$$

where: (P_{Dr}) is the pressure drop at the third zone in the vicinity of the open section of the wellbore, and:

$$\delta = \frac{\sqrt{s/\eta_D}tanh[\sqrt{s/\eta_D}(x_{eD}-1)]}{y_{eD}\,\mathrm{M}_D} + s \quad (22)$$

First zone (open sections close to the wellbore)

This zone is determined by the porous media where the radial flow regime occurs. It extends between the wellbore and the border with the second zone i.e. $(\mathrm{h_D}/2)$ as it is depicted in Fig. (4). Reservoir fluids in this zone flow radially in the vertical plan towards the wellbore. The flow equation in the third zone is given by:

$$\frac{\partial^2 \bar{P}_{Dr}}{\partial r_D^2} + \frac{1}{r_D}\frac{\partial \bar{P}_{Dr}}{\partial r_D} + \frac{1}{h_D^2}\frac{\partial^2 \bar{P}_{Dr}}{\partial z_D^2} + \frac{\partial \bar{P}_{Do}}{\partial y_D}\Big|_{y_D=h_D/2} - s\bar{P}_{Dr} = 0.0 \quad (23)$$

The boundary conditions of the first zone in the vertical plan are:

$$\frac{\partial \bar{P}_{Dr}}{\partial z_D}\Big|_{z_D=0.0} = 0.0 \quad (24)$$

$$\frac{\partial \bar{P}_{Dr}}{\partial z_D}\Big|_{z_D=h_D} = 0.0 \quad (25)$$

while the boundary condition in the horizontal plan are:

$$\frac{\partial \bar{P}_{Dr}}{\partial r_D}\Big|_{r_D=h_D/2} = 0.0 \quad (26)$$

$$r_D\frac{\partial \bar{P}_{Dr}}{\partial r_D}\Big|_{r_D=r_{wD}} = -\frac{1}{s} \quad (27)$$

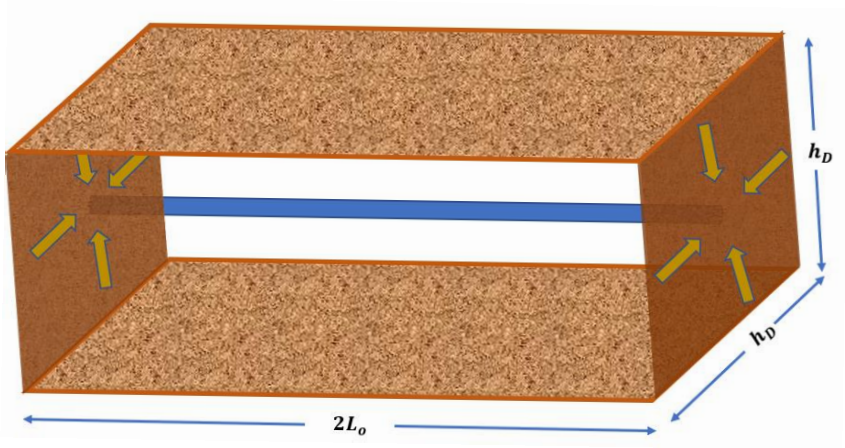

Figure 4 First zone (the vicinity of the open section of the wellbore).

Eq. (23) can be solved for the pressure drop inside the wellbore (P_{wD}) where ($r_D = r_{wD}$) using the abovementioned boundary conditions.

$$P_{wD} = \frac{1}{2sr_{wD}} \int_{-1}^{1} \sum_{n=0.0}^{n=\infty} \left[\frac{K_1(h_D\sqrt{\mathcal{E}})I_0(r_D\sqrt{\mathcal{E}}) + K_0(r_D\sqrt{\mathcal{E}})I_1(h_D\sqrt{\mathcal{E}})}{\sqrt{\mathcal{E}}K_1(r_{wD}\sqrt{\mathcal{E}})I_1(h_D\sqrt{\mathcal{E}}) - \sqrt{\mathcal{E}}K_1(h_D\sqrt{\mathcal{E}})I_1(r_{wD}\sqrt{\mathcal{E}})} \right] cos(n\pi z_D) cos(n\pi z_{wD}) d\alpha \quad (28)$$

where:

$$r_D = (x_D - \alpha) \quad (29)$$

$$\mathcal{E} = \left(\frac{n\pi}{h_D}\right)^2 + \beta \quad (30)$$

$$\beta = \sqrt{\delta} tanh\left[\sqrt{\delta}(y_{eD} - h_D/2)\right] + s \quad (31)$$

More details about the solutions of the flow equations in the three zones are given in Appendix-B.

Pressure behaviors

The impact of the closed sections on the pressure behavior of horizontal wellbores has been studied for different reservoir configurations, wellbore lengths, closed section lengths, and different petrophysical properties of closed and open sections. Fig. (5a, b) represents the pressure behavior and pressure derivative of short horizontal wellbores depleting square reservoirs of ($x_{eD} = y_{eD} = 2.0$). The wellbore length of the two cases is ($L_D = L_w/h = 40.0$). Fig. (5a) exhibits the pressure and pressure derivative of different open and closed section lengths when the petrophysical properties of the two sections are similar ($\eta_D = 1.0$) while the petrophysical properties of the closed sections in Fig. (5b) is different than those in the open section ($\eta_D = 0.001$) i.e. the permeability of the closed sections is much less than the open section. The following comments are inferred from these two figures:

1- The pressure drop at early production time increases significantly when the closed section length increases. Physically, this can be understood as the cross-section area of flow decreases when the closed section length increases. However, the impact of the closed section length is not significant at late production time.

2- The observed flow regimes when the porous media of the open and closed section have the same petrophysical properties are different than those observed when different petrophysical properties exist in the open and closed sections. For the first case, early radial, linear, and pseudo-steady state flow regimes are very well developed, while the bi-linear flow regime is not developed very well. It is seen, in Fig. (5a), for a very short time after linear flow regime and before pseudo-steady state flow regime. Nevertheless, the bi-linear flow regime is very well developed for the second case, Fig. (5b), while the linear flow regime is observed for a short time. The difference in the petrophysical properties of the second case helps developing the bi-linear flow regime because reservoir fluids move very slowly in the porous media of the closed sections (third zone).

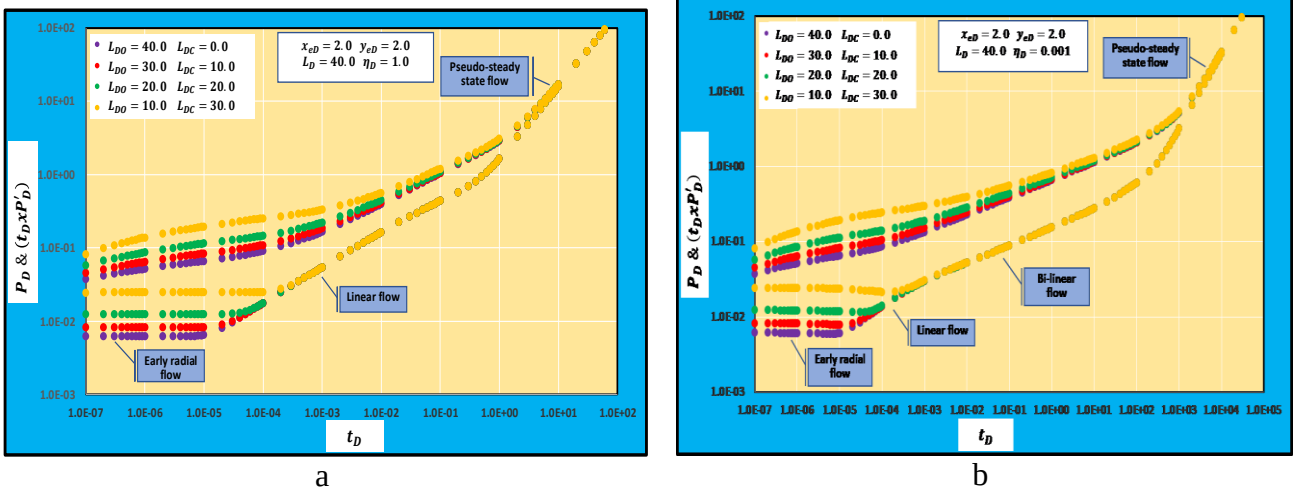

a b

Figure 5 Pressure and pressure derivative behaviors of short horizontal wellbores with different closed section lengths, (a) Similar petrophysical properties of open and closed section (b) Different petrophysical properties.

3- Pseudo-steady state is reached faster when the petrophysical properties of the porous media of open and closed sections are similar than the case of different properties because reservoir fluids move faster in the first case than the second where bad properties have existed in the closed sections.

4- The Bi-linear flow regime might not be observed when the wellbore does have only an open section while the linear flow regime might not be observed when the closed section is very long. For very long horizontal wellbores and long closed sections, the pressure behaviors could be similar to those seen for hydraulically fractured reservoirs where the bi-linear flow regime is the dominant in the porous media as it is depicted from Fig. (6a, b). This figure demonstrates the pressure and pressure derivative of very long wellbores ($L_D = 320.0$) that extend in rectangular drainage areas ($x_{eD} = 2.0, y_{eD} = 1.0$). Linear flow and bi-linear flow regimes are the dominant flow regimes in the porous media of similar and different petrophysical properties while early radial flow regime might not be observed or could be observed for a very short time at early production. Developing the early radial flow regime and the time elapsed by this flow regime depend on the formation thickness (h_D).

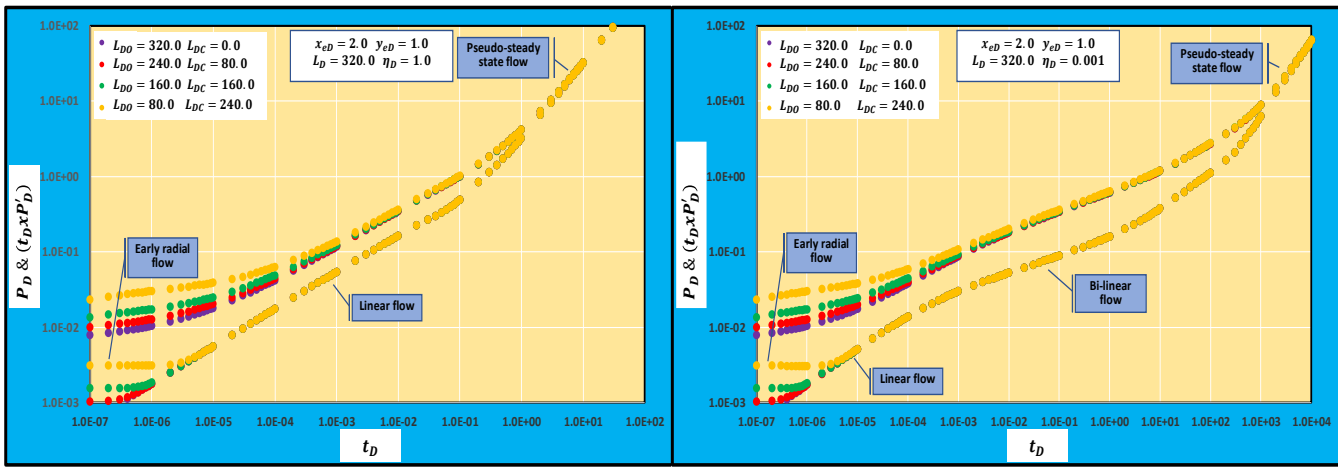

Figure 6 Pressure and pressure derivative behaviors of very long horizontal wellbores with different closed section lengths, (a) Similar petrophysical properties of open and closed section (b) Different petrophysical properties.

For the same wellbore length ($L_D = 40.0$) used to deplete big square drainage areas ($x_{eD} = y_{eD} = 8.0$), the pseudo-radial flow regime is seen very clear after linear flow regime and before pseudo-steady state flow regime regardless of the length of the closed sections when the petrophysical properties are similar in porous media of open and closed sections as it is exhibited in Fig. (7a). However, this flow regime is not very well developed after the bi-linear flow regime when the petrophysical properties of the open and closed sections are different as shown in Fig. (7b).

For long horizontal wellbores ($L_D = 160.0$) depleting square drainage areas ($x_{eD} = y_{eD} = 2.0$), the pressure and pressure derivative behaviors are similar to those resulting from short wellbores except that the early radial flow regime may not last for a long production time as demonstrated by Fig. (8a, b). These behaviors are seen for the two cases of similar and different petrophysical properties of open and closed sections. The time elapsed by the early radial flow regime could be longer when the closed sections are longer than the short closed sections.

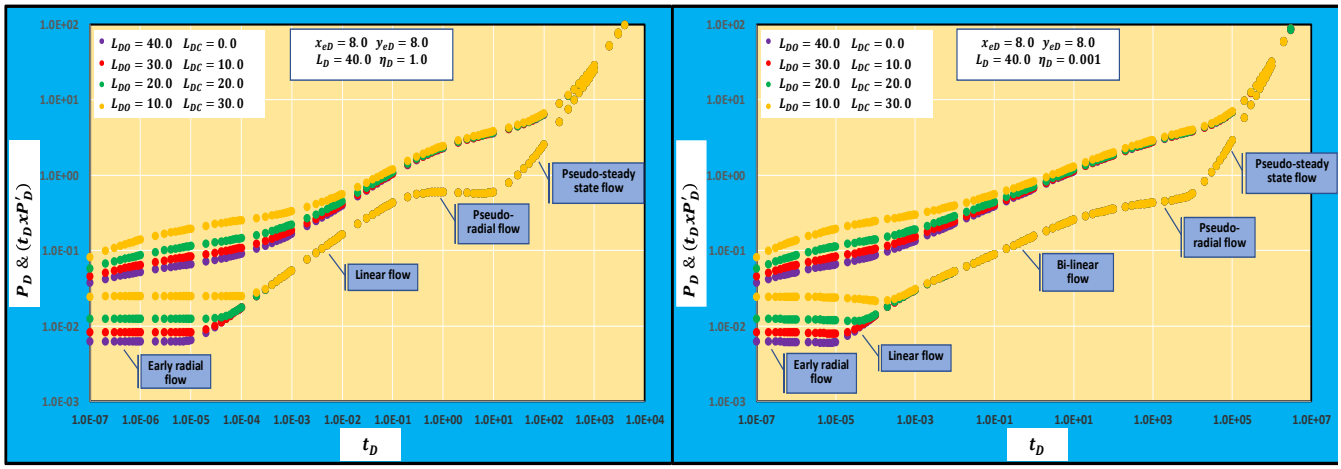

a b

Figure 7 Pressure and pressure derivative behaviors of short horizontal wellbores in big drainage areas with different closed section lengths, (a) Similar petrophysical properties of open and closed section (b) Different petrophysical properties.

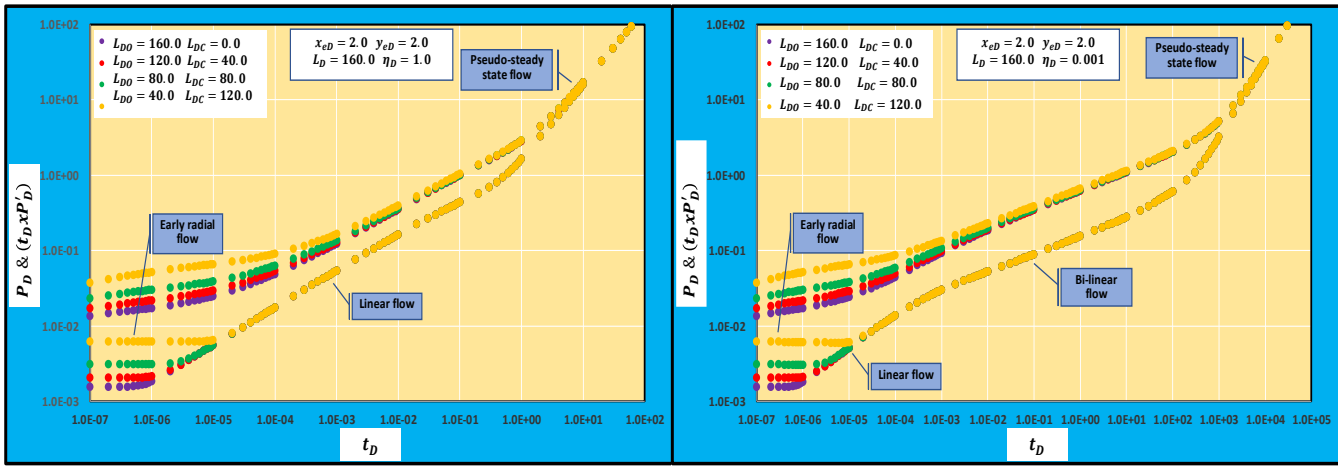

a b

Figure 8 Pressure and pressure derivative behaviors of long horizontal wellbores with different closed section lengths, (a) Similar petrophysical properties of open and closed section (b) Different petrophysical properties.

Flow regimes

It is very well documented that the main flow regimes that could be observed when the reservoirs are depleted by horizontal wellbores are early radial, linear, and pseudo-steady state flow regimes. Pseudo-radial flow regime might be developed also when the drainage areas are big and the wellbores are short. In this study, bi-linear is a new flow regime that is observed when parts of the wellbore are left close and the petrophysical properties of the closed sections are not similar to those in the open sections. The analytical models of the pressure and pressure derivative of early radial, linear, pseudo-radial, and pseudo-steady state flow regimes have been presented and documented very well in the literature. Therefore, the focus of this study is given only to the new bi-linear flow regime.

Bi-linear flow regime represents the simultaneous linear flow of reservoir fluids from the porous media of closed sections to the porous media of the open sections close to the reservoir boundary and from this section to the porous media in the vicinity of the wellbore as it is shown in Fig. (9). This flow regime is very well developed when there is a big difference between the petrophysical properties of closed and open section porous media. It appears after linear flow regime and before pseudo-steady state flow regime if pseudo-radial flow regime is not developed. It is characterized by a straight line of slope $(1/4)$ on the pressure derivative curves. The analytical models of the bi-linear flow regime have been developed in this study using the results of the pressure and pressure derivatives. These models, in the dimensionless form, are:

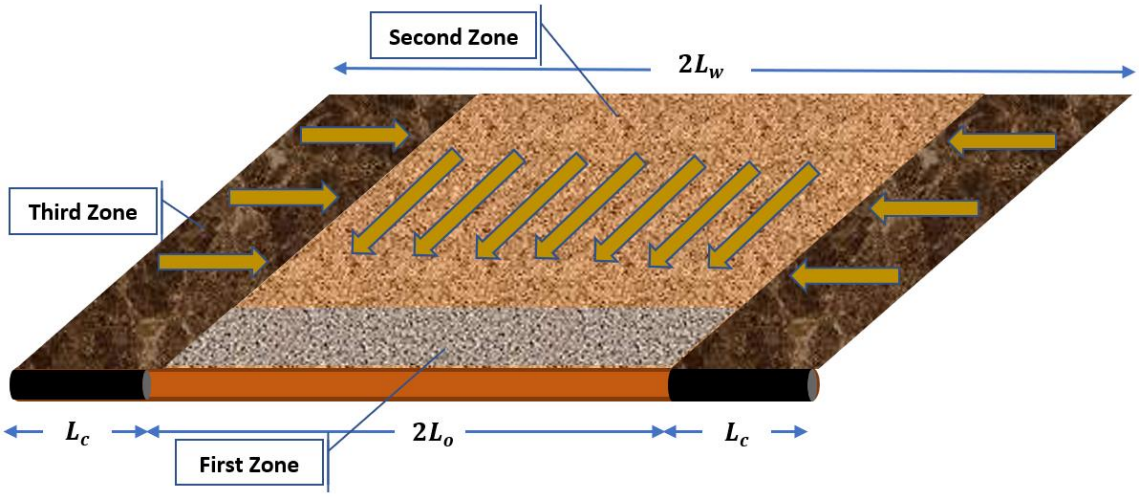

Figure 9 Schematic drawing for bi-linear flow regime.

$$(t_D x P'_D)_{BLF} = \frac{(\pi t_D)^{1/4}}{8} \quad (32)$$

$$(P_D)_{BLF} = \frac{(\pi t_D)^{1/4}}{2} + s_{BLF} \quad (33)$$

The subscript (BLF) means the bi-linear flow regime. The term (s_{BLF}) is the skin factor of the bi-linear flow regime. The comparison between the pressure and pressure derivative calculated by Eq. (28) and the pressure and pressure derivate calculated by Eqs. (32), and (33) is shown in Fig. (10).

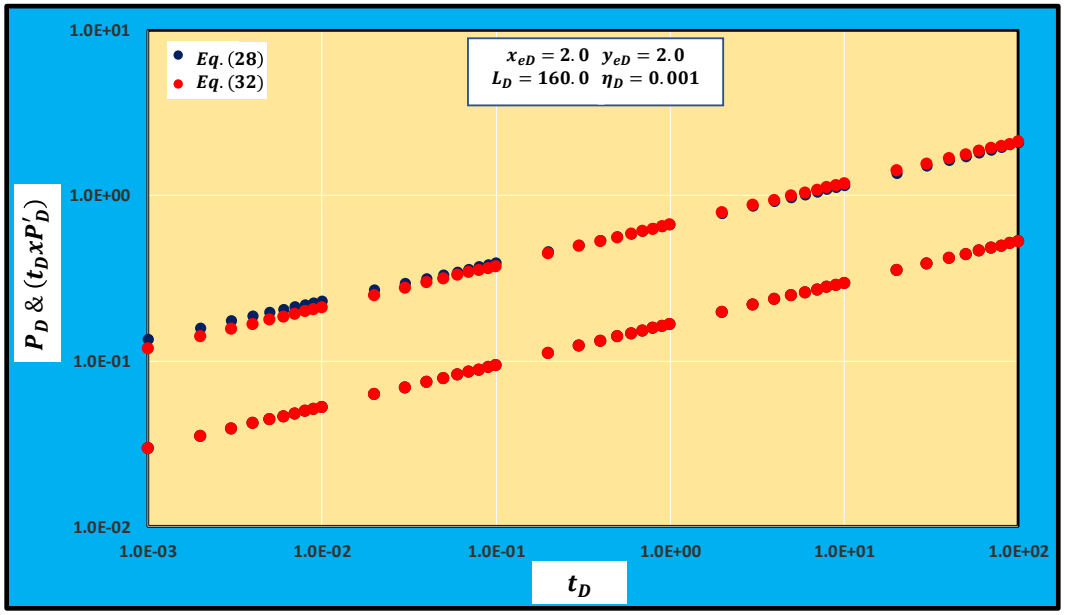

Figure 10 Comparison of pressure and pressure derivative of Eq. (28) and Eqs. (32), and (33).

Eqs. (32), and (33) can be solved for oil reservoirs using field units as follows:

$$(\mathrm{tx}\Delta \mathrm{P}'_{\mathrm{wf}})_{\mathrm{BLF}} = 3.0\frac{\mathrm{q}\mu \mathrm{B}_{\mathrm{o}}}{\mathrm{k}_{\mathrm{o}}\mathrm{h}\sqrt{\mathrm{L}_{\mathrm{o}}}}\left(\frac{\mathrm{k}}{\emptyset \mu \mathrm{c}_{\mathrm{t}}}\right)_{\mathrm{o}}^{1/4}\sqrt[4]{\mathrm{t}} \quad (34)$$

$$(\Delta P_{wf})_{BLF} = 12.0\frac{q\mu B_o}{k_o h\sqrt{L_o}}\left(\frac{k}{\emptyset\mu c_t}\right)_o^{1/4}\sqrt[4]{t} + \frac{141.2q\mu B_o}{k_o h}s_{BLF} \quad (35)$$

Eqs. (34), and (35) suggest that plotting the pressure drop inside the wellbore and its derivative versus production time on a log-log plot yields two straight lines of a slope $(1/4)$. The pressure derivative corresponds to a production time of $(1.0\ hr)$ can be used to characterize the porous media in the vicinity of the wellbore or to check the efficiency of the open section length (L_o). Similarly, the skin factor of the bi-linear flow regime can be calculated using the same production time and the corresponding pressure drop.

$$L_o = \left[3.0\frac{q\mu B_o}{k_o h(tx\Delta P'_{wf})_{1.0hr}}\left(\frac{k}{\emptyset\mu c_t}\right)_o^{1/4}\right]^2 \quad (36)$$

$$s_{BLF} = \frac{k_o h}{141.2q\mu B_o}\left[(\Delta P_{wf})_{1.0hr} - 12.0\frac{q\mu B_o}{k_o h\sqrt{L_o}}\left(\frac{k}{\emptyset\mu c_t}\right)_o^{1/4}\right] \quad (37)$$

The starting time of the bi-linear flow regime is a function of the open section length and its petrophysical properties. It can be estimated from the following model:

$$t_{sBLF} = 1.2\left(\frac{\emptyset\mu c_t}{k}\right)_o L_o^2 \quad (38)$$

The time when this flow regime is terminated could be estimated for small drainage area where pseudo-steady state flow regime follows bi-linear flow regime using the following model:

$$t_{eBLF} = 1.9 * 10^3\left(\frac{\emptyset\mu c_t}{k}\right)_o L_o^2 \quad (39)$$

while this time for big drainage area where pseudo-radial flow regime is developed after bi-linear flow regime is calculated by:

$$t_{eBLF} = 3.0 * 10^5\left(\frac{\emptyset\mu c_t}{k}\right)_o L_o^2 \quad (40)$$

Productivity index

The productivity index is well defined mathematically as the amount of oil or gas that can be produced at the surface by applying a pressure drop of (1.0 psi) inside the wellbore. It has different behaviors with production time based on the flow conditions that could dominate in the porous media whether transient or pseudo-steady state. During transient state flow conditions, the productivity index may decrease sharply while it can be assumed constant during pseudo-steady state flow conditions unless the well conditions progressively deteriorate because of the formation damage and skin factor (Diyashev and Economides, 2006). For a constant production rate, the productivity index, in dimensionless form, during transient state flow is calculated by:

$$J_D = \frac{1}{P_{wD}} \quad (41)$$

while it is calculated during pseudo-steady state flow by:

$$J_D = \frac{1}{P_{wD} - 2\pi t_{DA}} \quad (42)$$

The real-time productivity index for oil reservoirs, for example, can be calculated from the dimensionless productivity index, calculated by Eqs. (41), and (42) using:

$$J = \frac{k_o h}{141.2\mu B_o} J_D \quad (43)$$

Similar to the pressure behavior, the impact of the closed sections of horizontal wellbores is seen at early and intermediate production time when the transient state is the dominant flow condition in the porous media while very little or no impact at late production time is observed when pseudo-steady sate flow conditions have reached. This impact is demonstrated by Figs. (10a, b), and (11a, b) for short and long horizontal wellbores respectively with different open and closed section lengths for similar and different petrophysical properties. From these two figures, the following conclusions have been reached:

1- The maximum impact of closed sections is observed at early production time when the early radial flow regime dominates the porous media in the vicinity of the open section of the wellbore (First zone). This impact decreases when linear flow regime, the flow from the porous media of the open section close to the reservoir boundary (Second zone), is developed and becomes very slight when the bi-linear flow regime dominates in the porous media of the open (Second zone) and closed sections (Third zone). When the pseudo-steady state flow regime is reached at late production time, the impact of the closed sections is not clearly seen.

2- The length of the closed sections significantly affects the productivity index at early production time when reservoir fluids undergo transient state flow conditions. The longer closed sections give the lower productivity index compared to the fully open horizontal wellbores as shown in Fig. (13a). This is true as the pressure drop inside the wellbore increases when the length of the closed sections increases. It is very clear from this figure that the productivity index during the

early radial flow regime is not affected by the difference in the petrophysical properties of the porous media of open and closed sections. This is also true as the flow of reservoir fluids during this flow regime comes from the first zone or the porous media in the vicinity of the open section of the wellbore only i.e. the production pulse has not reached the second and third zone of the drainage area. It is important to emphasize that the productivity indices in Fig. (13a) are all taken at the same dimensionless production time. Fig. (13a) suggests a linear relationship between the wellbore length and the productivity index and a linear relationship between the impact of the closed sections on the productivity index and the index itself.

3- Bi-linear flow regime exhibits a sharp decrease in the productivity index with the production time compared to the productivity index behavior during the early radial flow regime. This would indicate the sharp increase in the pressure drop inside the wellbore during this flow regime. This behavior is similar to the productivity index behavior when the linear flow regime is developed for the case of similar petrophysical properties of the porous media of open and closed section wellbores.

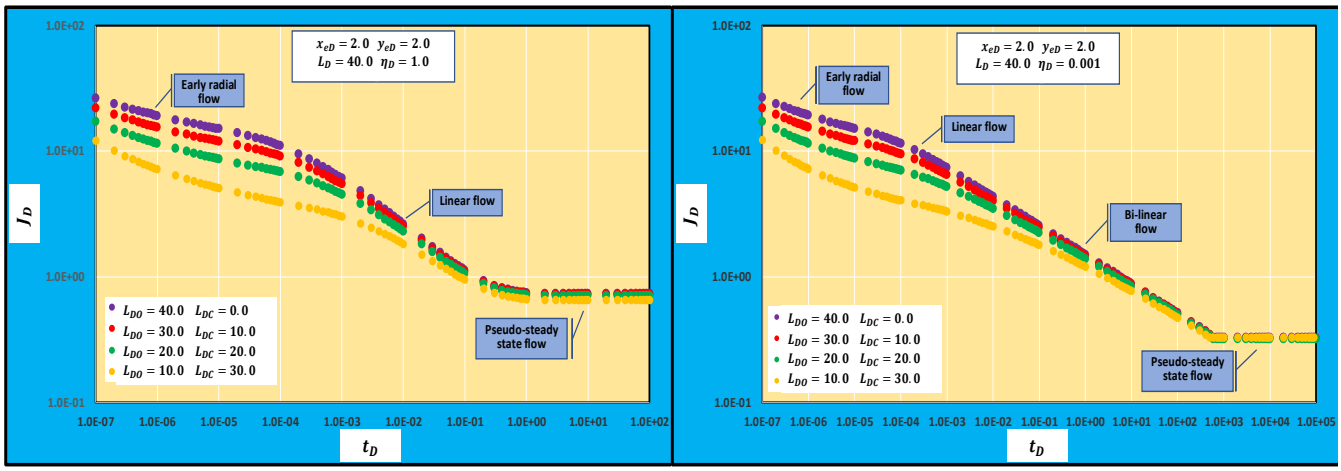

a b

Figure 11 : Productivity index behaviors of short horizontal wellbores with different closed section lengths, (a) Similar petrophysical properties of open and closed section (b) Different petrophysical properties.

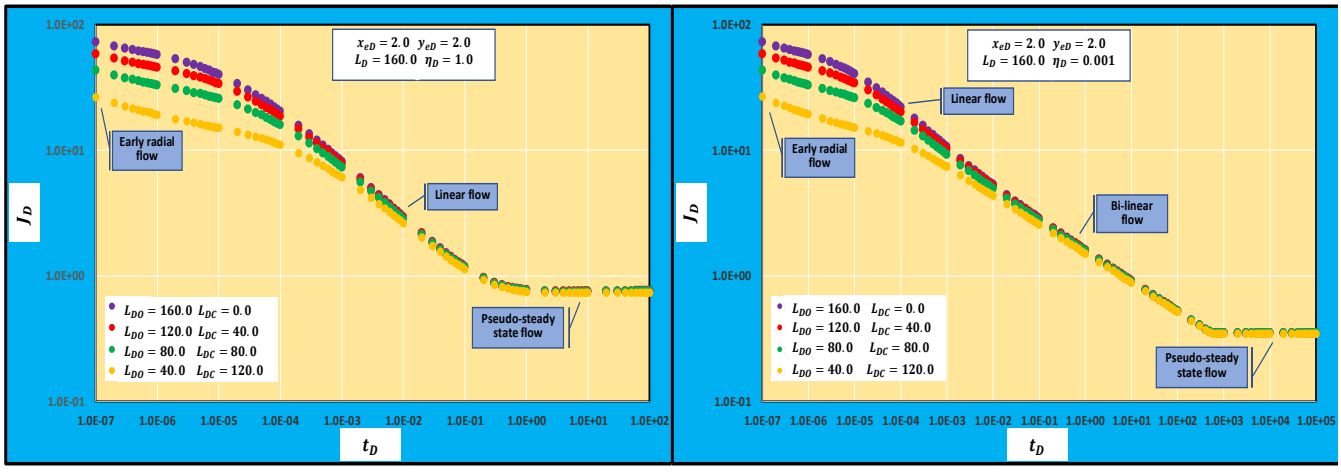

a b

Figure 12 Pressure and pressure derivative behaviors of long horizontal wellbores with different closed section lengths, (a) Similar petrophysical properties of open and closed section (b) Different petrophysical properties.

4- Stabilized pseudo-steady state productivity index when the petrophysical properties of the porous media of open and closed sections are different is less than the index when the porous media of the two sections are similar as it is depicted in Fig. (13d). The reason for that is the high pressure drop required for reservoir fluids to flow from the porous media of the closed sections that are characterized by bad petrophysical properties compared to the porous media of the open section. However, the productivity index of bi-linear and linear flow regime when the petrophysical properties of the

porous media are different is greater than the index of the bi-linear and linear flow regimes of similar properties of the porous media as can be seen in Fig. (13b) and (13c), while the productivity index of early radial flow regime is the same for the different and similar petrophysical properties of the porous media of open and closed sections of the wellbores as it is shown in Fig. (13a). Dislike the early radial flow regime, the relationship between the productivity index and wellbore length and closed section length is close to being a logarithmic relationship rather than a linear relationship.

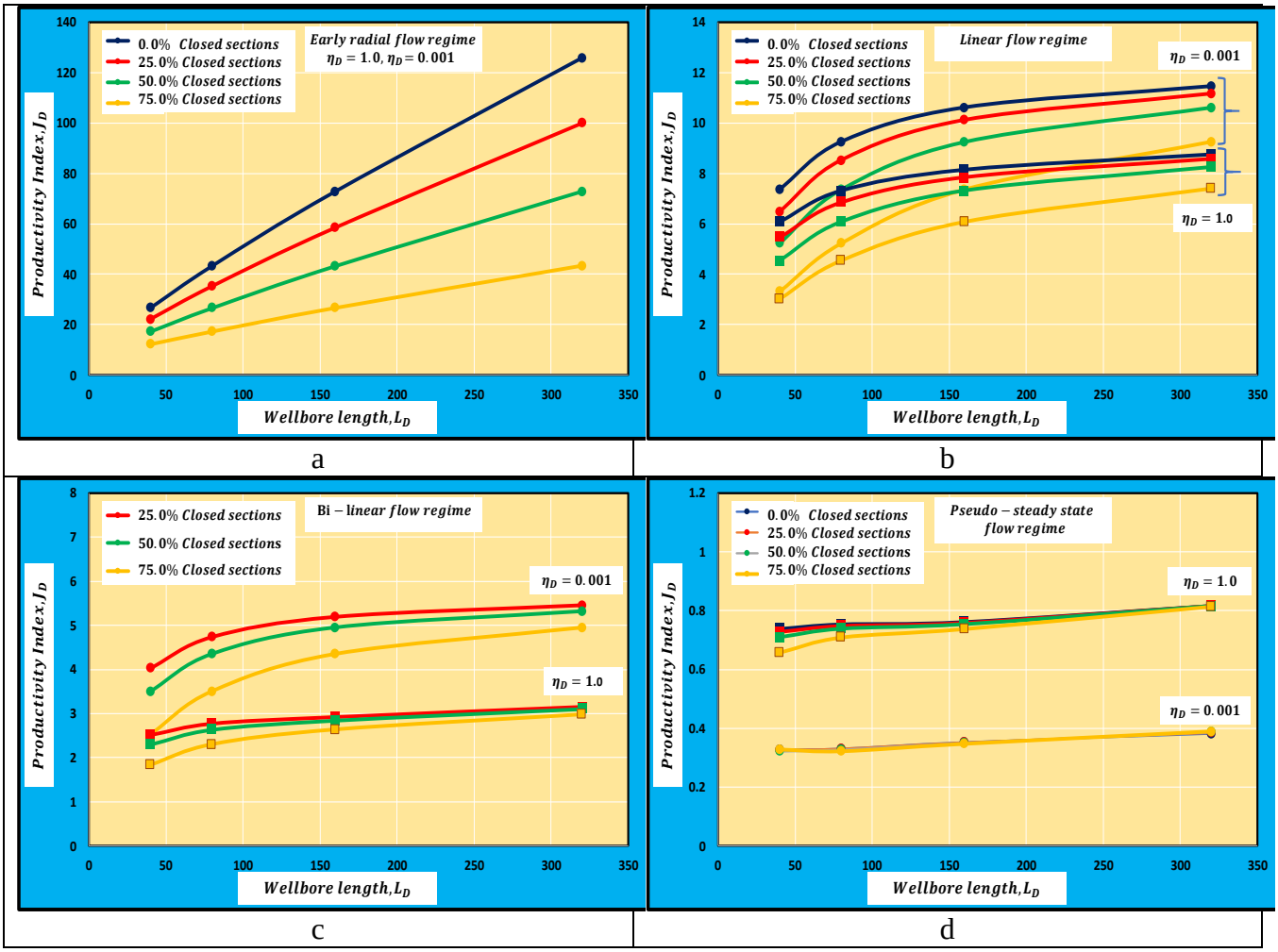

Figure 13 Productivity index of a horizontal wellbore acting in square drainage area (x_eD=y_eD=2.0) for different flow regimes, (a) Early radial flow regime (b) Linear flow regime (c) Bi-linear flow regime (d) Pseudo-steady state floe regime.

6- Verifications

The proposed approach in this study has been verified by the comparison with the well-known approaches presented and published in the literature. The first verification is made by the comparison with the results obtained from the single segments' models presented by Gringarten and Ramey 1973, Ozkan 1988, and Daviau et al. 1988. The reservoir and fluid properties used in the verification are listed in Table-1. The dimensionless parameters used in the verification are:

$$x_{eD} = 2.0 \quad y_{eD} = 2.0 \quad L_D = 10.0 \quad h_D = 0.1 \quad r_{wD} = 0.002 \quad L_{Do} = 10.0 \quad L_{Dc} = 0.0$$

Table 1 Reservoir and fluid properties.

Reservoir length, x_e, ft	1000.0
Reservoir width, y_e, ft	1000.0
Reservoir thickness, h, ft	50.0
Wellbore half-length, L_w, ft	500.0
Open section half-length, L_o, ft	500.0
Closed section length, L_c, ft	0.0
Petrophysical properties coefficient, η_D	1.0
Wellbore radius, r_w, ft	1.0

The results of the proposed models show an excellent matching with the results obtained by the models presented by Gringarten and Ramey 1973, Ozkan 1988, and Daviau et al. 1988 as it can be seen in Fig. (14). However, this verification does not consider the impact of the closed sections on the pressure behavior as the three previously introduced models dealt with fully open horizontal wellbores only with no segmentation. It shows only how the proposed models could give accurate results when they are adjusted for the applications of regular horizontal wellbores without closed sections.

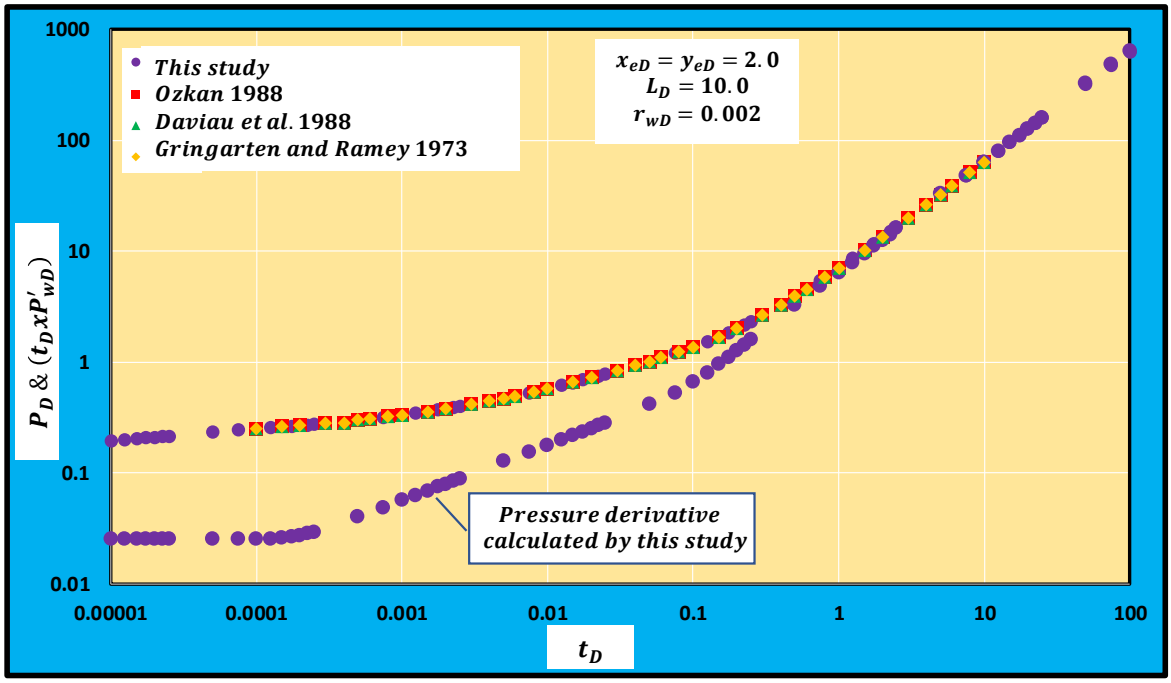

Figure 14 Comparison between the proposed models in this study and previously introduced models.

The second verification is made by the comparison of the productivity index calculated by the proposed models in this study and the index calculated by the model presented by Goode and Wilkinson 1991. Reservoir and fluid properties that have been used by Goode and Wilkinson 1991, shown in Table-2, are used in the second verification.

Table 2 Reservoir and fluid properties, Goode and Wilkinson 1991.

Reservoir length, x_e, ft	4000.0
Reservoir width, y_e, ft	2000.0
Reservoir thickness, h, ft	400.0
Wellbore half-length, L_w, ft	500.0
Open section half-length, L_o, ft	500.0
Closed section length, L_c, ft (Case-3)	400.0
Petrophysical properties coefficient, η_D	1.0
Wellbore radius, r_w, ft	0.345

The pressure, pressure derivative, and productivity index have been calculated and plotted, as shown in Fig. (14a, b), using the data given in Table-2 using the proposed models in this study for two cases; fully open wellbore and 80% closed sections. Two equal-length closed sections are located at the toe and heel of the wellbore (Case-3 in Goode and Wilkinson 1991). The petrophysical properties of the open and closed sections are assumed similar. Fig. (14b) indicates that the dimensionless stabilized productivity index of the fully open horizontal wellbore is (0.3675) while it is (0.1057) for the 80% closed sections. Therefore, the normalized productivity index of the 80% closed sections to the fully open wellbore is (0.288). This result is very close to the normalized productivity index shown in Fig. (15b) for $(L_{1/2}/L_x = 0.125)$.

The normalized productivity index has been calculated for different reservoir lengths and plotted versus the reciprocal of reservoir length $(1/x_{eD})$ as demonstrated in Fig. (15a). The results are very close to the results obtained by Goode and Wilkinson 1991.

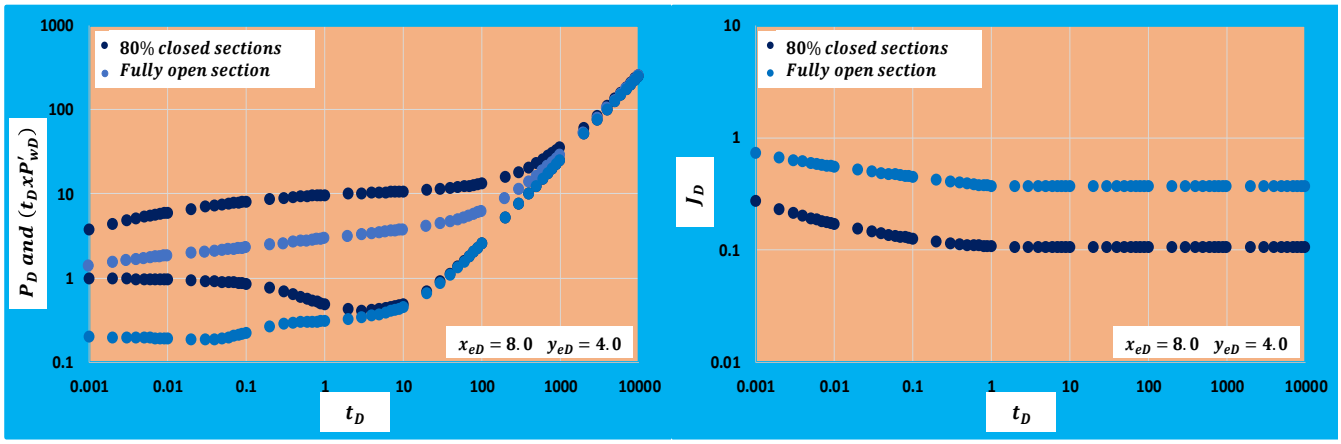

a b

Figure 15 (a) Pressure and pressure derivate behavior (b) Productivity index behavior.

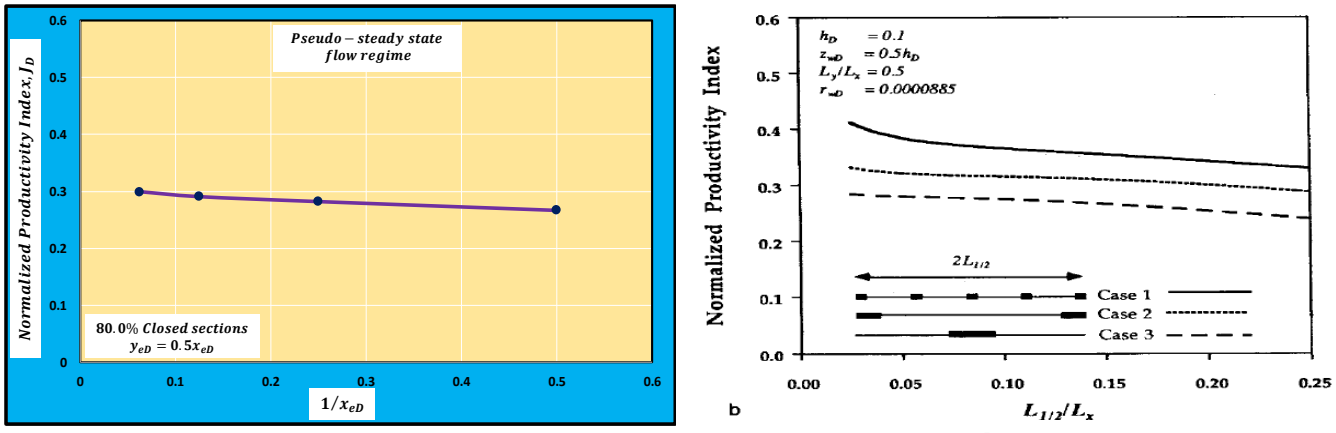

a b

Figure 16 Comparison between the normalized pseudo-steady state productivity index calculated by (a) the proposed models in this study (b) Goode and Wilkinson 1991.

The third verification is made by examining the proposed models for long horizontal wellbores with long closed sections. Gringarten et al. 1974, and Spivak 1988 stated that the pressure behavior of hydraulically fractured reservoirs could be similar to unfractured reservoirs depleted by long horizontal wellbores. Hydraulically fractured reservoirs are characterized by the dominance of three flow regimes; linear, bi-linear, and pseudo-steady state flow regimes. The first represents the flow of reservoir fluid inside hydraulic fractures linearly towards the wellbore. The second represents the simultaneous linear flow from the stimulated reservoir volume (SRV) between adjacent fractures towards the fractures themselves and the flow inside these fractures towards the wellbore. While the third one represents reservoir boundary-dominated flow regime. It is also true that hydraulically fractured reservoirs may have two porous media with different petrophysical properties. The first is the porous media between fractures where the fracturing process could enhance the permeability and the second is the pours media beyond the fracture tips and extend to the reservoir boundaries where the permeability might not be affected by the fracturing process (Al-Rbeawi 2017).

For a long horizontal wellbore ($L_D = 320.0$) with an equal length of open and closed sections as shown in Fig. (16), the open section of the wellbore analogs very wide hydraulic fracture. To minimize the early time elapsed by the early radial flow regime, the formation is assumed to have a short thickness ($h = 20$ ft). The petrophysical property coefficient of the closed and open sections is ($\eta_D = 0.001$). The pressure and pressure derivative of the wellbore are calculated and plotted in Fig. (17). It is very clear that three flow regimes are observed. The first is the linear flow regime that develops at early production time and represents the flow from the open section close to the reservoir boundary toward the open section close to the wellbore. The porous media of the open section close to the wellbore is very small so that the early radial flow regime may develop for a very short production time that is not noticeable. This flow regime is similar to the hydraulic fracture linear flow regime when reservoir fluids flow inside hydraulic fractures towards the wellbore. The second is the bi-linear flow regime that represents the flow from the closed section to the open section close to the reservoir boundary and the flow from this section to the open section in the vicinity of the wellbore. It is similar to the bi-linear flow regime of hydraulically fractured reservoirs. The third is the pseudo-steady state flow regime that is similar in reservoirs depleted by horizontal wellbore and hydraulic fractures.

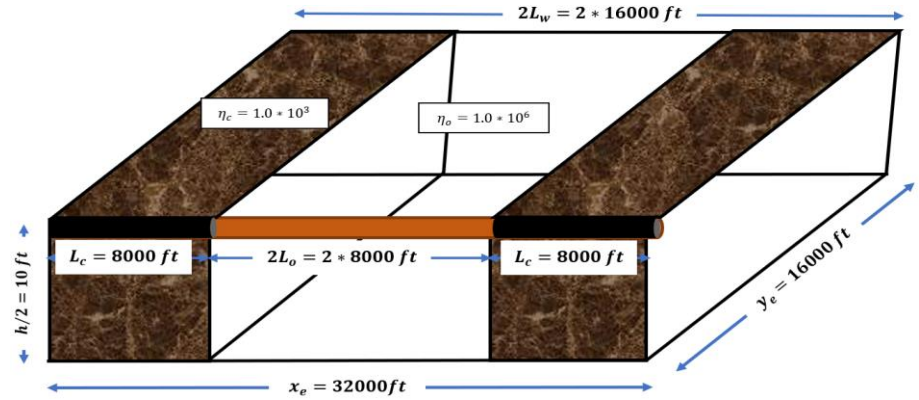

Figure 17 Long horizontal wellbore with long closed sections.

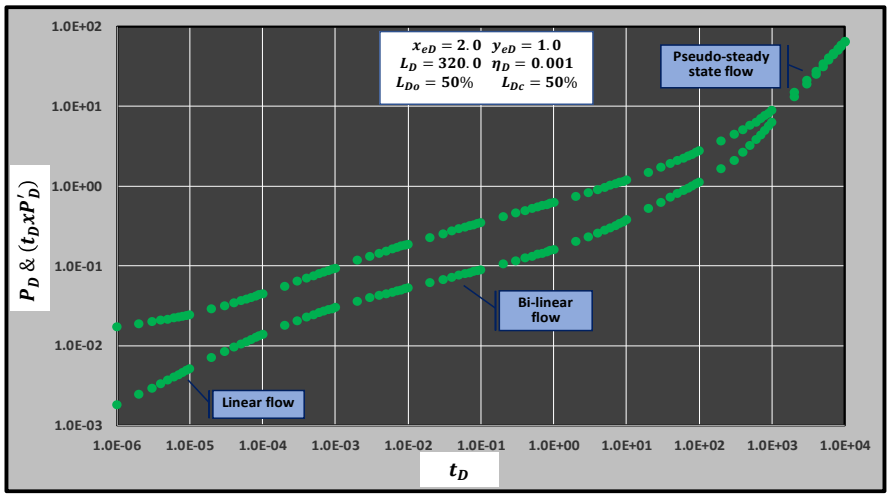

Figure 18 Pressure and pressure derivative behavior of long horizontal wellbore.

Conclusions

New analytical models have been developed in this study for the pressure behavior and productivity index of horizontal wellbores that are partially completed. These models consider three porous media with different petrophysical properties and different flow regimes. The first is the open section in the vicinity of the wellbore where the radial flow regime is developed while the second is the porous media of the open section close to the reservoir boundary where the linear flow regime dominates the flow of reservoir fluid. The third is the porous media of the closed sections where the bi-linear flow regime is observed. The following conclusions have been reached:

1-The closed sections of the horizontal wellbores may have a significant impact on the pressure behavior and productivity index, especially at early production time. This impact decreases during intermediate production time and becomes insignificant at late production time.

2-A new bi-linear flow regime is observed when the wellbore is partially completed. It is not seen when the wellbore is fully open to flow. This flow regime is very well developed and lasts for a long time when the petrophysical properties of open and closed sections are sharply different. New analytical models for the pressure and pressure derivative of this flow regime have been developed and can be used to characterize the porous media in the closed and open sections.

3-The pressure behavior and flow regimes of the reservoirs depleted by very long horizontal wellbores with closed sections are similar to those developed when the reservoirs are depleted by hydraulic fractures.

4-The productivity index of the early radial flow regime is more affected by the closed sections but it is not affected by the difference in the petrophysical properties between open and closed sections. This is physically understood as the early radial flow regime occurs when reservoir fluids flow from the porous media in the vicinity of the wellbore only i.e. the production pulse has not reached the porous media of the closed sections where different petrophysical properties could have existed.

5-The productivity index of linear and bi-linear flow regimes is impacted by the closed section length and the difference in petrophysical properties of open and closed sections. This index decreases with the length of the closed sections but increases with the increase of the difference in the petrophysical properties of open and closed sections.

6-The stabilized pseudo-steady state productivity index is not significantly impacted by the closed section length; however, it is impacted by the difference in the petrophysical properties of open and closed sections. Dislike linear and bi-linear flow regimes, this index decreases with the increase of the difference in the petrophysical properties of open and closed sections.

Nomenclatures

B_o	Oil formation volume factor
c_t	Formation total compressibility, psi^{-1}
h	Formation thickness, ft
h_D	Dimensionless formation thickness
K_o	Bessel function $K-$ type of zero $-$ order
K_1	Bessel function of $K-$ type of the first order
I_o	Bessel function of $I-$ type of zero $-$ order
I_1	Bessel function of $I-$ type of the first order

k_0	Permeability of open section porous media, md
k_c	Permeability of closed section porous media, md
J_D	Productivity index, dimensionless
j	Productivity index, (STB/day)/psi
L_D	Dimensionless wellbore length
L_{Do}	Dimensionless open section wellbore length
L_{Dc}	Dimensionless closed section wellbore length
L_c	Closed section wellbore length, ft
L_o	Open section half wellbore length, ft
L_w	Half wellbore length, ft
P_{wf}	Bottom hole flowing pressure drop, psi
P_D	Pressure drop, dimensionless
P_{Dc}	Closed section pressure drop, dimensionless
P_{Do}	Open section (close to reservoir boundary) pressure drop, dimensionless
P_{Dr}	Open section (close to the wellbore) pressure drop, dimensionless
P_c	Closed section pressure drop, psi
P_o	Open section (close to reservoir boundary) pressure drop, psi
P_r	Open section (close to the wellbore) pressure drop, psi
P_{wD}	Bottom hole flowing pressure, dimensionless
ΔP	Pressure drop, psi
ΔP_{wf}	Bottom hole pressure drop, psi
q	Flow rate, STB/day
r	Radius, ft
r_D	Dimensionless radius
r_w	Wellbore radius, ft
r_{wD}	Dimensionless wellbore radius
s	Laplace operator
t	Time, hrs
t_D	Time, dimensionless
t_{DA}	Dimensionless time based on drainage area
$(t_D x P'_D)$	Pressure derivative, dimensionless
$(t_D x P'_{wD})$	Bottom hole flowing pressure derivative, dimensionless
$(t x P'_{wf})$	Bottom hole flowing pressure derivative
x	X − coordinate of a point in the porous media
x_e	Reservoir boundary, ft
x_w	X − coordinate of a wellbore
x_D	X − coordinate of a point in the porous media, dimensionless
x_{eD}	Reservoir length, dimensionless
x_{wD}	X − coordinate of a wellbore, dimensionless
y	Y − coordinate of a point in the porous media
y_e	Reservoir boundary, ft
y_w	Y − coordinate of a wellbore
y_D	Y − coordinate of a point in the porous media, dimensionless
y_{eD}	Reservoir width, dimensionless
y_{wD}	Y − coordinate of a wellbore, dimensionless
z	Z − coordinate of a point in the porous media
z_w	Z − coordinate of a wellbore
z_D	Z − coordinate of a point in the porous media, dimensionless
z_{wD}	Z − coordinate of a wellbore, dimensionless
μ	Viscosity, cp
∅	Porosity
α	Integration dummy variable

References

[1] Abbasy, Imran, Ritchie, Barry, Pitts, Michael, White, Brendan, and M. Rushdan Jaafar, 2010. Challenges in Completing Long Horizontal Wells Selectively. SPE Drilling & Completion 25 (02). doi.org/10.2118/116541-PA

[2] Al-Rbeawi, S., 2017. How much stimulated reservoir volume and induced matrix permeability could enhance unconventional reservoir performance. Journal of Natural Gas Science and Engineering, 46(2017). doi.org/10.1016/j. jngse.2017.08.017

[3] Al-Rbeawi S.; Tiab, D., 2012. Interpretation of pressure transient test of horizontal wells with multiple hydraulic fractures and zonal isolations. PhD thesis, University of Oklahoma, Norman, Ok, USA.

[4] Daviau, F., Mouronval, G., Bourdarot, G., & Curutchet, P.,1988. Pressure Analysis for Horizontal Wells. SPE Formation Evaluation, 3 (04). doi:10.2118/14251-PA

[5] Diyashev, I. R, & Economides, M. J., 2006. The Dimensionless Productivity Index as a General Approach to Well Evaluation. SPE Production & Operation Journal, 21 (03). doi:10.2118/94644-PA.

[6] Eriksen, Jan Hilding, Sanfilippo, Francesco, Kvamsdal, Arne L., Flint, George, and Erling Kleppa. Orienting Live Well Perforating Technique Provides Innovative Sand-Control Method in the North Sea. SPE Drilling & Completion 16 (03). doi.org/10.2118/73195-PA

[7] Frick, T. P., Brand, C. W., Schlager, B., and M. J. Economides, 1995. Horizontal Well Testing of Isolated Segments. SPE Journal,1 (03). doi.org/10.2118/29959-PA

[8] Gangle, F. J., Schultz, K. L., McJannet, G. S., and N. Ezekwe, 1995. Improved Oil Recovery Using Horizontal Wells at Elk Hills, California. SPE Drilling & Completion Journal 10 (01). doi.org/10.2118/27884-PA

[9] Goode, P.A., and D.J. Wilkinson, 1991. Inflow Performance of Partially Open Horizontal Wells. Journal of Petroleum Technology, 43 (08). doi.org/10.2118/19341-PA

[10] Gringarten, Alain C., and Henry J. Ramey, 1973. The Use of Source and Green's Functions in Solving Unsteady-Flow Problems in Reservoirs. SPE Journal 13 (05). doi.org/10.2118/3818-PA

[11] Gringarten, Alain C., Ramey, Henry J., and R. Raghavan, 1974. Unsteady-State Pressure Distributions Created by a Well with a Single Infinite-Conductivity Vertical Fracture. SPE Journal, 14 (04). doi.org/10.2118/4051-PA

[12] Hillestad, Eivind, Skillingstad, Paal, Folse, Kent, Hjorteland, Oyvind, and Janne Hauge. Novel Perforating System Used in North Sea Results in Improved Perforation for Sand Management Strategy. Paper presented at the SPE Annual Technical Conference and Exhibition held in Houston, Texas, USA, Sep. 26-29. doi.org/10.2118/90164-MS

[13] Horn, M. J., Plathey, D. P., and Ouahiba Ibrahim, 1998. Multilateral Horizontal Well Increases Liquids Recovery in the Gulf of Thailand. SPE Drilling & Completion Journal, 13 (02). doi.org/10.2118/38065-PA

[14] Kostøl, Petter, and Knut Østvang, 1995. Completion and Workover of Horizontal and Extended-Reach Wells in the Statfjord Field. SPE Drilling & Completion Journal 10 (04). doi.org/10.2118/28559-PA

[15] Ozkan, E. 1988. Performance of horizontal wells. PhD dissertation, The University of Tulsa, Tulsa, Ok, USA.

[16] Ozkan, Erdal, Yildiz, Turhan, and Rajagopal Raghavan, 1999. Pressure-Transient Analysis of Perforated Slant and Horizontal Wells. Paper presented at the SPE Annual Technical Conference and Exhibition held in Houston, Texas, USA, Oct. 3-6. doi.org/10.2118/56421-MS

[17] Pucknell, J.K., and W.H. Broman, 1994. An Evaluation of Prudhoe Bay Horizontal and High-Angle Wells After 5 Years of Production. Journal of Petroleum Technology, 46 (02). doi.org/10.2118/26596-PA

[18] Rentano, Albertus and Muhammed Yamin, 1999. Impact of Completion Technique on Horizontal Well Productivity. SPE paper presented at the Asia and Pacific Oil and Gas Conference held in Jakarta, Indonesia. doi.org/10.2118/54302-MS

[19] Sadek, Hani, Williams, Charles R., and Michael Smith, 1998. Production Strategy Yields Unique Perforating, Cost-Efficient Multilateral Drilling Solution in the Beryl Field. Paper presented at the SPE Asia Pacific Oil and Gas Conference and Exhibition held in Perth, Australia, Oct. 12-14. doi.org/10.2118/50123-MS

[20] Seale, R., Athans, J., and D. Themig, 2007. An Effective Horizontal Well Completion and Stimulation System. Journal of Canadian Petroleum Technology, 46 (12). doi.org/10.2118/07-12-04

[21] Sognesand, Sigmund, Skotner, Peder, and Jan Hauge, 1994. Use of Partial Perforations in Oseberg Horizontal Wells. Paper presented at the SPE Annual Technical Conference and Exhibition, New Orleans, Louisiana, Oct. 25-27. doi.org/10.2118/28569-MS

[21] Sognesand, Sigmund, 1996. Evaluation of Oseberg Horizontal Wells After Four Years Production. Paper presented at the European Petroleum Conference, Milan, Italy, Oct. 22-24. doi.org/10.2118/36864-MS

[22] Spivak, David, 1988. Pressure analysis for horizontal wells. PhD dissertation submitted to Louisiana Tech University.

[23] Thomson, D. W., and M. F. Nazroo, 1998. Design and Installation of a Cost-Effective Completion System for Horizontal Chalk Wells Where Multiple Zones Require Acid Stimulation. SPE Drilling & Completion Journal, 13 (03). doi.org/10.2118/51177-PA

[24] Tronvoll, Johan, Eek, Arne, Larsen, Idar, and Francesco Sanfilippo, 2004. The Effect of Oriented Perforations as a Sand Control Method: A Field Case Study from the Varg Field, North Sea. Paper presented at the SPE International Symposium and Exhibition on Formation Damage Control held in Lafayette, Louisiana, USA, February 18-20. 2004. doi.org/10.2118/86470-MS

[25] Yildiz, Turhan, 2004. Inflow Performance Relationship for Perforated Horizontal Wells. SPE Journal, 9 (03). doi.org/10.2118/88987-PA

[26] Yildiz, Turhan, 2006. Productivity of Selectively Perforated Horizontal Wells. SPE Production & Operation Journal, 21 (01). doi.org/10.2118/90580-PA

Appendix-A: Dimensionless parameters

$$h_D = \frac{h}{L_w} \quad \text{(A-1)}$$

$$L_D = \frac{L_w}{h} \quad \text{(A-2)}$$

$$L_{Do} = \frac{L_o}{h} \quad \text{(A-3)}$$

$$L_{Dc} = \frac{L_c}{h} \quad \text{(A-4)}$$

$$P_D = \frac{k_o \Delta P}{141.2 q \mu B_o} \quad \text{for oil reservoirs} \quad \text{(A-5)}$$

$$r_D = \frac{r}{L_w} \quad \text{(A-6)}$$

$$r_{wD} = \frac{r_w}{L_w} \quad \text{(A-7)}$$

$$t_D = \frac{0.0002637\, k_o t}{(\emptyset \mu c_t)_o L_o^2} \quad \text{(A-8)}$$

$$t_{DA} = \frac{0.0002637\, k_o t}{(\emptyset \mu c_t)_o A} \quad \text{(A-9)}$$

$$x_D = \frac{x}{x_e} \quad \text{(A-10)}$$

$$x_{eD} = \frac{x_e}{L_w} \quad \text{(A-11)}$$

$$x_{wD} = \frac{x_w}{x_e} \quad \text{(A-12)}$$

$$y_D = \frac{y}{y_e} \quad \text{(A-13)}$$

$$y_{eD} = \frac{y_e}{L_w} \quad \text{(A-14)}$$

$$y_{wD} = \frac{y_w}{y_e} \quad \text{(A-15)}$$

$$z_D = \frac{z}{h} \quad \text{(A-16)}$$

$$y_{wD} = \frac{z_w}{h} \quad \text{(A-17)}$$

Appendix-B: Mathematical formulation

The flow equations of the porous media depleted by horizontal wellbores with closed sections have been solved for the three zones separately:

1- First zone-The porous media of the closed sections:

This part of porous media is shown in Fig. (B-1). Reservoir fluids in this part linearly flow towards the open section of the porous media close to reservoir boundary and there is no flow from this section to the wellbore. The flow equation of this section is given by:

$$\frac{\partial^2 P_c}{\partial x^2} = \frac{(\emptyset \mu c)_c}{k_c} \frac{\partial P_c}{\partial t} \quad \text{(B-1)}$$

In dimensionless form:

$$\frac{\partial^2 P_{Dc}}{\partial x_D^2} = \frac{1}{\eta_D} \frac{\partial P_{Dc}}{\partial t_D} \quad \text{(B-2)}$$

where:

$$\eta_D = \frac{\eta_c}{\eta_0} \quad \text{(B-3)}$$

$$\eta_o = \frac{k_o}{(\emptyset \mu c_t)_o} \quad \text{(B-4)}$$

$$\eta_c = \frac{k_c}{(\emptyset \mu c_t)_c} \quad \text{(B-5)}$$

Using Laplace domain, Eq. (B-2) becomes:

$$\frac{\partial^2 \bar{P}_{Dc}}{\partial x_D^2} = \frac{s}{\eta_D} \bar{P}_{Dc} \tag{B-6}$$

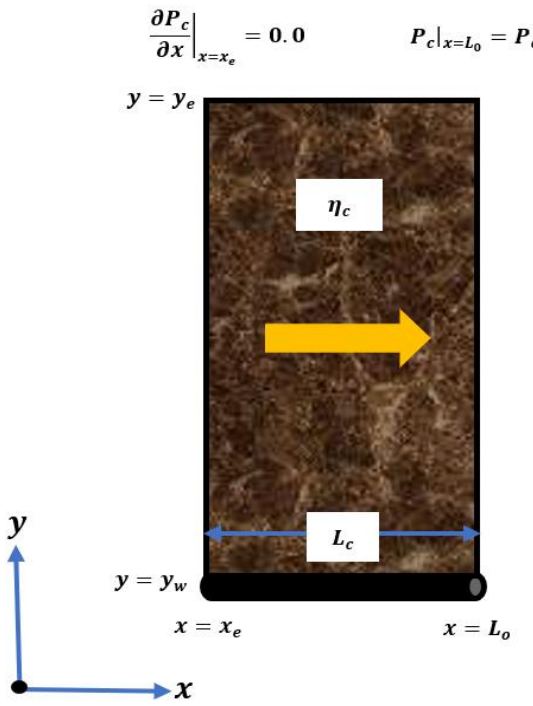

Figure B-1: Closed section porous media.

The boundary conditions, shown in Fig. (B-1), can be written in the Laplace domain also as follows:

$$\left(\frac{\partial \bar{P}_{Dc}}{\partial x_D}\right)_{x_D = x_{eD}} = 0.0 \tag{B-7}$$

$$\bar{P}_{Dc}|_{x_D=1.0} = \bar{P}_{Dc}|_{x_D=1.0} \tag{B-8}$$

and can be used to solve Eq. (B-6):

$$\bar{P}_{Dc} = \bar{P}_{Do}|_{x_D=1.0} \frac{cosh[\sqrt{s/\eta_D}(x_{eD} - x_D)]}{cosh[\sqrt{s/\eta_D}(x_{eD} - 1)]} \tag{B-9}$$

2- Second zone-Porous media close to reservoir boundary:

This part represents the porous media of the open section close to the reservoir boundary as shown in Fig. (B-2). It receives reservoir fluids from the closed sections and delivers them to the porous media close to the wellbore. Reservoir fluids in this part flow linearly toward the open section porous media close to the wellbore. The flow equation of this part is given by:

$$k_o \frac{\partial^2 P_o}{\partial y^2} + \frac{k_c}{(y_e - h/2)} \frac{\partial P_c}{\partial x}\Big|_{x=L_0} = (\emptyset \mu c_t)_o \frac{\partial P_o}{\partial t} \tag{B-10}$$

In dimensionless form, the model is:

$$\frac{\partial^2 P_{Do}}{\partial y_D^2} + \frac{1}{y_{eD} M_D} \frac{\partial P_{Dc}}{\partial x_D}\Big|_{x_D=1.0} = \frac{\partial P_{Do}}{\partial t_D} \tag{B-11}$$

and using Laplace domain, Eq. (B-11) is:

$$\frac{\partial^2 \bar{P}_{Do}}{\partial y_D^2} + \frac{1}{y_{eD} M_D} \frac{\partial \bar{P}_{Dc}}{\partial x_D} = s \bar{P}_{PDS} \tag{B-12}$$

where:

$$M_D = \frac{k_c}{k_0(y_{eD}-h_D/2)} \quad \text{(B-13)}$$

From Eq. (B-9), knowing that:

$$\left.\frac{\partial P_{Dc}}{\partial x_D}\right|_{x_D=1.0} = -\bar{P}_{Do}\sqrt{s/\eta_D}\,tanh\left[\sqrt{s/\eta_D}\,(x_{eD}-1)\right] \quad \text{(B-14)}$$

and substituting in Eq. (B-12):

$$\frac{\partial^2 \bar{P}_{Do}}{\partial y_D^2} - \delta \bar{P}_{Do} = 0.0 \quad \text{(B-15)}$$

where:

$$\delta = s + \frac{\sqrt{s/\eta_D}tanh\left[\sqrt{s/\eta_D}(x_{eD}-1)\right]}{y_{eD}M_D} \quad \text{(B-16)}$$

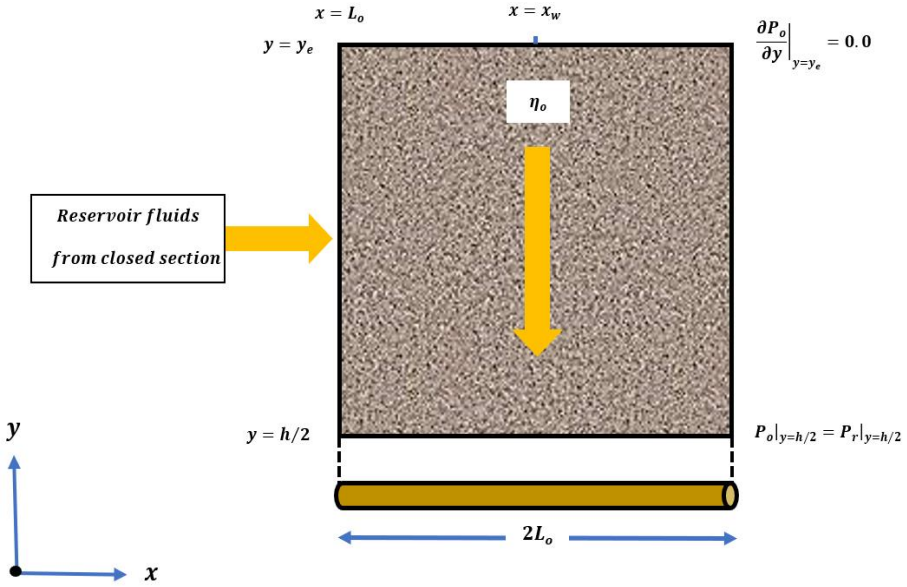

Figure B-2: Open section porous media close to the reservoir boundary.

Using the boundary conditions shown in Fig. (B-2):

$$\left(\frac{\partial \bar{P}_{Do}}{\partial y_D}\right)_{y_D=y_{eD}} = 0.0 \quad \text{(B-17)}$$

$$\bar{P}_{Do}|_{y_D=h_D/2} = \bar{P}_{Dr}|_{y_D=h_D/2} \quad \text{(B-18)}$$

Eq. (B-15) can be solved to:

$$\bar{P}_{Po} = \bar{P}_r|_{y_{eD}=h_D/2}\frac{cosh\left[\sqrt{\delta}(y_{eD}-y_D)\right]}{cosh\left[\sqrt{\delta}(y_{eD}-h_D/2)\right]} \quad \text{(B-19)}$$

3- **Third zone-Open section porous media in the vicinity of the wellbore:**

This part represents the porous media of the open section close to the wellbore as shown in Fig. (B-3). It is assumed that the petrophysical properties of this section are the same as the petrophysical properties of the open section porous media close to the reservoir boundary i.e. the formation damage or stimulation is not considered. The dominant flow regime in this section is the radial flow regime in the vertical plan towards the wellbore. The radius of the cylinder in this case equals half formation thickness $(h/2)$. The flow equation of this section is given by:

$$\frac{\partial^2 P_r}{\partial r^2}+\frac{1}{r}\frac{\partial P_r}{\partial r}+\frac{1}{h^2}\frac{\partial^2 P_r}{\partial z^2}+\frac{\partial P_o}{\partial y}\Big|_{y=h/2}=\frac{(\emptyset\mu c_t)_0}{k_0}\frac{\partial P_r}{\partial t} \quad \text{(B-20)}$$

In dimensionless form:

$$\frac{\partial^2 P_{Dr}}{\partial r_D^2}+\frac{1}{r_D}\frac{\partial P_{Dr}}{\partial r_D}+\frac{1}{h_D^2}\frac{\partial^2 P_{Dr}}{\partial z_D^2}+\frac{\partial P_{D0}}{\partial y_D}\Big|_{y_D=h_D/2}=\frac{\partial P_{Dr}}{\partial t_D} \quad \text{(B-21)}$$

In Laplace domain, Eq. (B-21) becomes:

$$\frac{\partial^2 \bar{P}_{Dr}}{\partial r_D^2}+\frac{1}{r_D}\frac{\partial \bar{P}_{Dr}}{\partial r_D}+\frac{1}{h_D^2}\frac{\partial^2 \bar{P}_{Dr}}{\partial z_D^2}+\frac{\partial \bar{P}_{D0}}{\partial y_D}\Big|_{y_D=h_D/2}=s\bar{P}_{Dr} \quad \text{(B-22)}$$

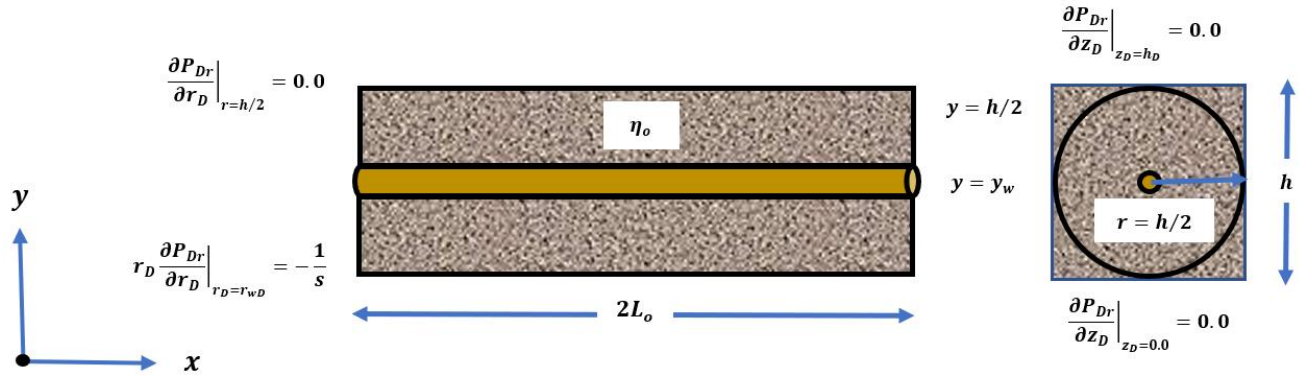

Figure B-3: Open section porous media in the vicinity of the wellbore.

Using Eq. (B-19):

$$\frac{\partial \bar{P}_{Do}}{\partial y_D}\Big|_{y_D=h_D/2}=-\bar{P}_{PDr}\sqrt{\delta}\,tanh\left[\sqrt{\delta}(y_{eD}-h_D/2)\right] \quad \text{(B-23)}$$

and substitute in Eq. (B-22):

$$\frac{\partial^2 \bar{P}_{Dr}}{\partial r_D^2}+\frac{1}{r_D}\frac{\partial \bar{P}_{Dr}}{\partial r_D}+\frac{1}{h_D^2}\frac{\partial^2 \bar{P}_{Dr}}{\partial z_D^2}-\beta\bar{P}_{Dr}=0.0 \quad \text{(B-24)}$$

where:

$$\beta=s+\sqrt{\delta}\,tanh\left[\sqrt{\delta}(y_{eD}-h_D/2)\right] \quad \text{(B-25)}$$

To solve Eq. (B-24), assuming:

$$\bar{P}_{Dr}=\bar{R}_{rD}\bar{Z}_{zD} \quad \text{(B-26)}$$

Eq. (B-24) becomes:

$$\bar{R}_{rD}^{"}\bar{Z}_{zD}+\frac{1}{r_D}\bar{R}_{rD}'\bar{Z}_{zD}+\frac{1}{h_D^2}\bar{R}_{rD}Z_{zD}^{"}-\beta\bar{R}_{rD}\bar{Z}_{zD}=0.0 \quad \text{(B-27)}$$

and it can be written as:

$$h_D^2\left(\frac{\bar{R}_{rD}^{"}+\frac{1}{r_D}\bar{R}_{rD}'-\beta\bar{R}_{rD}}{\bar{R}_{rD}}\right)=-\frac{\bar{Z}_{zD}^{"}}{\bar{Z}_{zD}}=\lambda \quad \text{(B-28)}$$

Eq.(B-28) can be divided into two equations:

$$\bar{R}_{rD}^{"}+\frac{1}{r_D}\bar{R}_{rD}'-\mathcal{E}\bar{R}_{rD}=0.0 \quad \text{(B-29)}$$

where:

$$\mathcal{E}=\beta+\lambda \quad \text{(B-30)}$$

and:

$$\bar{Z}''_{zD} - \lambda \bar{Z}_{zD} = 0.0 \quad \text{(B-31)}$$

Eq. (31) can be solved to:

$$\bar{Z}_{zD} = Ccos\left(\sqrt{\lambda} z_D\right) + Dsin\left(\sqrt{\lambda} z_D\right) \quad \text{(B-32)}$$

and using the boundary conditions shown in Fig. (B-3):

$$\left(\frac{\partial \bar{P}_{Dr}}{\partial z_D}\right)_{z_D=0.0} = 0.0 \quad \text{(B-32)}$$

$$\left(\frac{\partial \bar{P}_{Dr}}{\partial z_D}\right)_{z_D=h_D} = 0.0 \quad \text{(B-33)}$$

Eq. (B-32) can be solved to:

$$\bar{Z}_{zD} = \frac{1}{2}\cos\left(\sqrt{\lambda} z_D\right) cos\left(\sqrt{\lambda} z_{wD}\right) \quad \text{(B-34)}$$

where:

$$\lambda = (n\pi)^2 \qquad n \geq 0.0 \quad \text{(B-35)}$$

while Eq. (B-29) can be solved to:

$$\bar{R}_{rD} = AI_o\left(r_D\sqrt{\mathcal{E}}\right) + BK_o\left(r_D\sqrt{\mathcal{E}}\right) \quad \text{(B-36)}$$

and using the boundary conditions shown in Fig. (B-3):

$$\left(\frac{\partial \bar{P}_{Dr}}{\partial r_D}\right)_{r_D=h_D/2} = 0.0 \quad \text{(B-37)}$$

$$\left(\frac{\partial \bar{P}_{Dr}}{\partial x_D}\right)_{r_D=r_{wD}} = -\frac{1}{s} \quad \text{(B-38)}$$

Eq. (B-36) can be solved to:

$$\bar{R}_{rD} = \frac{1}{sr_{wD}\sqrt{\mathcal{E}}}\left[\frac{K_1(h_D/2\sqrt{\mathcal{E}})I_o(r_D\sqrt{\mathcal{E}}) + K_o(r_D\sqrt{\mathcal{E}})I_1(h_D/2\sqrt{\mathcal{E}})}{K_1(r_{wD}\sqrt{\mathcal{E}})I_1(h_D/2\sqrt{\mathcal{E}}) - K_1(h_D/2\sqrt{\mathcal{E}})I_1(r_{wD}\sqrt{\mathcal{E}})}\right] \quad \text{(B-39)}$$

Combining Eqs. (B-34), and (B-39) gives the dimensionless bottom hole pressure drop:

$$\bar{P}_{wD} = \frac{1}{2sr_{wD}\sqrt{\mathcal{E}}}\sum_{n=0.0}^{n=\infty}\int_{-1}^{1}\left[\frac{K_1(h_D/2\sqrt{\mathcal{E}})I_o(r_D\sqrt{\mathcal{E}}) + K_o(r_D\sqrt{\mathcal{E}})I_1(h_D/2\sqrt{\mathcal{E}})}{K_1(r_{wD}\sqrt{\mathcal{E}})I_1(h_D/2\sqrt{\mathcal{E}}) - K_1(h_D/2\sqrt{\mathcal{E}})I_1(r_{wD}\sqrt{\mathcal{E}})}\right]\cos\left(\sqrt{\lambda} z_D\right) cos\left(\sqrt{\lambda} z_{wD}\right) d\alpha \quad \text{(B-40)}$$

where:

$$r_D = \sqrt{(x_D - \alpha)^2 + y_D^2} \quad \text{(B-41)}$$

$$r_D = (x_D - \alpha) \qquad for\ y_D = 0.0 \quad \text{(B-42)}$$

Conversion factors

bbl x 1.589873	E-01=m^3
cp x 1.0	E-03=Pa.s
ft x 3.048	E-01=m
in x 2.54	E-00=cm
Psi x 6.894757	E+00=kPa
Ibm x 0.453592	E+00=Kg
md x 0.9869	E+11=cm^2